



HAL
open science

Cavity enhanced FTIR spectroscopy using a femto OPO absorption source

Xavier de Ghellinck d'Elseghem Vaernewijck, Keevin Didriche, Clement Lauzin, Atina Rizopoulos, Michel Herman, Samir Kassi

► **To cite this version:**

Xavier de Ghellinck d'Elseghem Vaernewijck, Keevin Didriche, Clement Lauzin, Atina Rizopoulos, Michel Herman, et al.. Cavity enhanced FTIR spectroscopy using a femto OPO absorption source. *Molecular Physics*, 2011, 109, pp.2173-2179. 10.1080/00268976.2011.602990 . hal-00722799

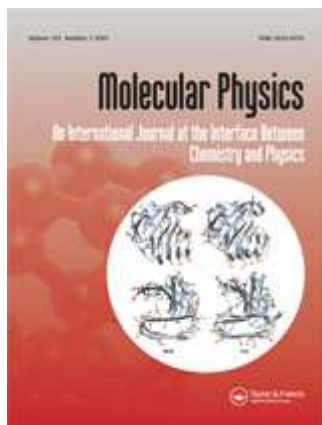
HAL Id: hal-00722799

<https://hal.science/hal-00722799>

Submitted on 4 Aug 2012

HAL is a multi-disciplinary open access archive for the deposit and dissemination of scientific research documents, whether they are published or not. The documents may come from teaching and research institutions in France or abroad, or from public or private research centers.

L'archive ouverte pluridisciplinaire **HAL**, est destinée au dépôt et à la diffusion de documents scientifiques de niveau recherche, publiés ou non, émanant des établissements d'enseignement et de recherche français ou étrangers, des laboratoires publics ou privés.



Cavity enhanced FTIR spectroscopy using a femto OPO absorption source

Journal:	<i>Molecular Physics</i>
Manuscript ID:	TMPH-2011-0137.R1
Manuscript Type:	Special Issue Paper - Dijon HRMS
Date Submitted by the Author:	24-Jun-2011
Complete List of Authors:	de Ghellinck D'Elseghem Vaernewijck, Xavier; Université Libre de Bruxelles, Chimie quantique et Photophysique Didriche, Keevin; Université Libre de Bruxelles, Chimie quantique et Photophysique LAUZIN, Clement; Université Libre de Bruxelles, Chimie quantique et Photophysique Rizopoulos, Atina; Université Libre de Bruxelles, Chimie quantique et Photophysique Herman, Michel; Université Libre de Bruxelles, Chimie quantique et Photophysique Kassi, Samir; Universite Joseph Fourier, Laboratoire Interdisciplinaire de Physique
Keywords:	Cavity enhanced absorption spectroscopy, FTIR, Femtosecond OPO comb spectroscopy, Femto-FT-CEAS

REVISED

Molecular Physics

Special issue for Di Lonardo

**Cavity enhanced FTIR spectroscopy using
a femto OPO absorption source.**

X. de Ghellinck d'Elseghem Vaernewijck*, K. Didriche, C. Lauzin,
A. Rizopoulos and M. Herman**

Chimie quantique et Photophysique CP160/09
Faculté des Sciences
Université Libre de Bruxelles (U.L.B.)
Av. Roosevelt, 50
B-1050, Bruxelles
Belgium

S. Kassi

Laboratoire Interdisciplinaire de Physique (UMR 5588 CNRS-UJF)
Université Joseph Fourier
BP 87 F-38402 Saint-Martin d'Hères
France

* FRIA researcher

** Postdoctoral Researcher (F.R.S.-FNRS)

Pages: 21

Figures: 8

Tables: 1

Send mail to Prof. M. Herman, mherman@ulb.ac.be

Abstract

The $\nu_1+\nu_3$ band of $^{12}\text{C}_2\text{H}_2$ was recorded using a high resolution continuous scan Fourier transform interferometer fitted with a femto OPO absorption source. Various experimental schemes were successfully implemented, including multipass absorption in a cell and also in a supersonic expansion, and cavity enhanced absorption. An optimal rms noise equivalent absorption of $2.2 \cdot 10^{-9} \text{ cm}^{-1} \text{ Hz}^{-1/2}$ per spectral element was reached in the latter case, corresponding to $\alpha_{\text{min}} = 1.5 \cdot 10^{-7} \text{ cm}^{-1}$. Performances are illustrated and discussed.

Keywords

Keywords: Cavity enhanced absorption spectroscopy; FTIR, Femtosecond OPO comb spectroscopy, Femto-FT-CEAS

1. Introduction

Michelson-type Fourier transform interferometers (FTIR) are widely used in high resolution molecular infrared spectroscopy since pioneering studies such as those by, in alphabetical order, Brault (1,2), Delbouille (3,4), Guelachvili (5,6), Johns (7,8), Kauppinen (9,10), Valentin (11,12), Winnewisser (13,14) and their co-workers. More recently, new types of absorption schemes were developed to increase the signal and boost the detection sensitivity with FTIR instruments. For instance brighter absorption sources were used, such as synchrotron radiation (15) and broadband femto lasers (16,17), with conventional single or multipass absorption cells. Others were based on conventional sources with high finesse cavities to perform cavity enhanced absorption spectroscopy (CEAS) (18). Attempts to combine laser sources with CEAS and FTIR detection were also reported. Successful experiments include FT-CRDS (19,20) and FT-ICLAS (for intracavity laser absorption spectroscopy) (21,22) schemes. In 2010 cavity enhanced FTIR spectroscopy using a femtosecond laser absorption source was also reported (23,24), which we labeled Femto-FT-CEAS. The cavity modes comb was locked onto the Ti:Sa femto laser comb (the so-called “magic point (MP) (25,26)), detecting *e.g.* at ULB O₂ present in the atmosphere between the mirrors of the high finesse cavity open to air (23). We wish to report here on attempts to repeat such experiments, now using a tunable femto OPO absorption source and acetylene, $\nu_1+\nu_3$ (the symmetric and antisymmetric CH

1
2
3 stretching vibrations, respectively) as molecular band. In section 2, the
4
5 successful use of a bright femto OPO absorption source for FTIR is presented,
6
7
8 using various multipass arrangements. A more refined high-finesse cavity
9
10 design is described in section 3 to achieve OPO-Femto-FT-CEAS.
11
12 Performances are further illustrated in the final section, which also concludes
13
14 the present “proofs of principles”-type report. **Although the present**
15
16 **experiments will not involve locking the cavity comb onto the femto comb and**
17
18 **are sometimes referred to as of integrated cavity output spectroscopy (ICOS)**
19
20 **type, the latter is often associated to cavity off-axis experiments which is not**
21
22 **the case here. We shall therefore keep using the more general CEAS**
23
24 **terminology.**
25
26
27
28
29
30
31
32
33
34
35
36
37

38 **2. Use of a femto OPO absorption source**

39
40 In our previous work,(23) a femto Ti:Sa source (Coherent Chameleon
41
42 ULTRA II) served as absorption source. This laser is a mode locked laser with
43
44 80MHz repetition rate and 140 fs laser pulse width. We have now used this
45
46 laser to pump an OPO module (Coherent PP810), allowing for broader
47
48 wavelength coverage towards the IR. In principle, the full range 1 - 3 μm is
49
50 available if one also accounts for the idler option. It is, however limited by
51
52 atmospheric water absorption which prevents laser operation in the lower IR
53
54
55
56
57
58
59
60

1
2
3 water bands. This problem also occurs in the NIR in specific ranges between
4
5 7000 and 7500 cm^{-1} , as demonstrated in Figure 1. This figure also illustrates
6
7 the typical bandwidth available for each experiment, which is about 90 cm^{-1}
8
9 FWHM in the range probed during the present experiments on acetylene
10
11 (1.47 – 1.53 μm). Each recording comes with a base line extending over the
12
13 full spectral range appearing in Figure 1. Thus the observed base line in the
14
15 Figure merges the noise of all individual recordings. We shall here mainly
16
17 focus on the lower energy region in Figure 1.
18
19
20
21
22
23
24
25

26 We first checked that the use of the OPO module was compatible with
27
28 the high resolution Bruker IFS120HR FTIR continuous acquisition
29
30 procedure. The success of these experiments is illustrated in Figure 2
31
32 presenting a spectrum of acetylene in a supersonic expansion, recorded at 3
33
34 10^{-2} cm^{-1} resolution (defined as $0.9/\text{maximum optical path difference}$). A
35
36 multipass optics made of two drilled gold mirrors was used, set to 25 passes
37
38 in the expansion produced using a circular nozzle (0.5 mm inner diameter),
39
40 the central hole in the mirrors allowing for light input and exit as previously
41
42 described in the literature (27). We have used the latest version of the
43
44 FANTASIO+ set-up (for “Fourier transform, tunable diode laser and mass
45
46 spectrometers interfaced to a supersonic expansion”) built at ULB to produce
47
48 jet-cooled acetylene. This set-up is described in the literature and not further
49
50 detailed (28,29). Precise experimental conditions are provided in the caption
51
52
53
54
55
56
57
58
59
60

1
2
3 of Figure 2. We checked that the gain in S/N is about one order of magnitude
4
5 compared to the use of a global absorption source, other experimental
6
7 conditions being identical.
8
9

10
11 In a second step we achieved multipass absorption in a room
12
13 temperature cavity. The cavity, 90 cm long, was identical to the one further
14
15 described in the next section. The off-axis CEAS design was set to reach
16
17 about 5 m absorption pathlength. The C_2H_2 , $\nu_1+\nu_3$ band was again recorded,
18
19 now under room temperature conditions. A spectral portion is presented in
20
21 Figure 3 (top). Sharp negative signals corresponding to saturated peaks were
22
23 removed (as in forthcoming Figures) by using a subroutine suppressing the
24
25 corresponding data points from the spectra, thus after Fourier transforming
26
27 the recorded interferogram. The theoretical spectrum also shown in this
28
29 figure (bottom) is calculated using the parameters from the global model by
30
31 **Amyay** et al. (30). The regular series of lines missing in the simulation from
32
33 6535 to 6510 cm^{-1} is due to $^{13}CH^{12}CH$ present in natural abundance in the
34
35 sample (2%). **The observation of this isotopologue is a nice illustration of the**
36
37 **quality of the experimental data.** The noise level reveals a minimal
38
39 absorbance of $5 \cdot 10^{-3}$, *i.e.* an absorption detection limit $\bullet_{min} = 10^{-5} cm^{-1}$.
40
41
42
43
44
45
46
47
48
49
50

51 In a third step, we attempted to perform **on-axis** CEAS in a room
52
53 temperature high finesse cavity. A major limitation was, however
54
55 encountered, compared to our previous Ti:Sa experiments (23). It indeed
56
57
58
59
60

turned out that the manufactured tuning mechanism involves a dispersion element that inherently adds chirp. This prevented us from efficiently locking together the cavity and OPO combs, thus from reaching the MP. **This problem was not encountered in previous experiments using only the Ti:Sa pump source (23) since there is no similar dispersion element as in the OPO.** As a result all experiments were performed outside from the MP, by scanning the cavity length using a piezoelectric actuator (PZT) (HPST 1000 modulator) as described in the next section.

3. CEAS experiments

The set-up for CEAS experiments is schematized in Figure 4. Broadband injection of a high-finesse cavity was achieved using a pair of lenses (L_1 and L_2 , $f = 50$ mm). The cavity was made of half inch output couplers (Layertec) stated to have 99.3 % reflectivity (CM_1 and CM_2). It corresponds to a finesse $\mathcal{F} = \frac{\pi\sqrt{R_1R_2}}{1-\sqrt{R_1R_2}} \geq 445$). The output cavity mirror was set on a PZT. The cavity was about 77 cm long and the PZT was permanently modulating the cavity length. In this way, cavity modes are jittering and on the average every laser mode is equally transmitted, leading to a smooth transmission spectrum. Conditions need to be adapted empirically by tuning the cell length to a slightly different value for each selected central

1
2
3 wavelength and for each sample conditions (pressure) to optimize this
4
5 fringing smoothing effect.
6
7

8 The laser beam was sent through a HoYag type optical Faraday
9
10 isolator (Thorlabs) before injection in the cavity, to avoid optical feedback in
11
12 the laser oscillator. This proved to be essential in the success of the
13
14 experiments.
15
16
17

18
19
20 The output laser beam was directed into the high resolution
21
22 continuous scanning FTIR equipped with an InGaAs diode detector. The
23
24 entrance FTIR iris aperture was set to 1.15 mm, *i.e.* larger than the laser
25
26 beam diameter, the latter being focused to 10 μm at the FTIR entrance, using
27
28 a 12.5 cm focal lens (L_3). Spectra are presented in Figures 5 and 6,
29
30 illustrating various features.
31
32
33
34
35
36
37

38 As shown in Figure 5, the modulation frequency of the PZT had to be
39
40 set as high as possible (20 kHz) to reduce the noise level. This figure presents
41
42 the same spectral range recorded using various PZT modulation frequencies.
43
44 The dominant contribution to the noise is actually likely to result from the
45
46 beat between various frequencies with similar values, namely from the laser
47
48 jitter, the PZT modulation and the FTIR sampling process. The resulting beat
49
50 is smoothed out due to the detector response time ($\sim 1\mu\text{s}$), actually lengthened
51
52 by the use of a lowpass frequency filter. This effect is more efficient if the PZT
53
54
55
56
57
58
59
60

1
2
3 modulation is higher. The remaining noise at 20 kHz PZT modulation, which
4 is channeling, can actually be removed from real spectra by producing a
5 transmittance signal, *i.e.* dividing by I_0 . It is likely that even higher
6 modulation will help in this problem. All other spectra presented here were
7 recorded using 20 kHz modulation frequency.
8
9
10
11
12
13
14
15
16
17

18 The effect of the FTIR resolution is illustrated in **Figure 6** with
19 spectra recorded with 0.04, 0.02, 0.01 and 0.005 cm^{-1} resolution, from bottom
20 to top. It is worth noting that a discretization of the spectrum starts
21 appearing at 0.02 cm^{-1} FTIR resolution and is well present at 0.005 cm^{-1}
22 FTIR resolution, giving rise to spike-like background signal. It is due to the
23 free spectral range (FSR) of the fixed laser comb (FSR = 80 MHz), limiting
24 the final resolution.
25
26
27
28
29
30
31
32
33
34
35
36
37

38 We also checked that S/N increases as the square root of the number of
39 scans (n) as expected for white noise.
40
41
42
43
44
45
46
47

48 **4. Data and conclusion**

49
50 We used optimal conditions to record the $\nu_1 + \nu_3$ band in C_2H_2 , as shown
51 on **Figure 7**. It corresponds to an optimal rms noise equivalent absorption of
52 $2.2 \cdot 10^{-9} \text{ cm}^{-1} \text{ Hz}^{-1/2}$ per spectral element, and a value \bullet_{\min} of $1.5 \cdot 10^{-7} \text{ cm}^{-1}$.
53
54
55
56
57
58
59
60

1
2
3 These values are about 60 times better than those for the off-axis CEAS
4
5 experiment previously reported (Figure 3). This improvement results from
6
7 the increase in pathlength (30 times improvement) and also (another factor of
8
9 2) from the new design, involving an optical isolator and the fine tuning of
10
11 the cavity, therefore decreasing the noise. This band and the many
12
13 accompanying bands in the range have already been investigated in the
14
15 literature using conventional FTIR multipass set-ups (e.g. (31-33)). Recently,
16
17 ultra high sensitivity cavity ring down spectroscopy (CRDS) was applied in
18
19 the range (30,34), revealing many more, weaker bands. The data recorded
20
21 using Femto-FT-CEAS are of intermediate quality. We could spot lines not
22
23 reported in the conventional FTIR investigations. Some of these were actually
24
25 not assigned in the CRDS data, yet. Taking advantage on the very precise
26
27 global modeling of the acetylene vibration-rotation energy levels in acetylene
28
29 available from the literature and of the accurate resulting spectral
30
31 simulations (30), we assigned low J -lines transitions in two bands, as
32
33 reported in Table 1. All lines in these bands correspond to weak transitions,
34
35 some overlapped by stronger lines and therefore missing in the Table. Some
36
37 of the lines are highlighted in Figure 8.

38
39
40
41
42
43
44
45
46
47
48
49
50
51 In conclusion, the experiments just reported demonstrate that Femto-
52
53 FT-CEAS can be successfully achieved using a tunable broadband OPO
54
55 source. Various limitations existing with our present set-up were highlighted,
56
57
58
59
60

1
2
3 as well as directions for improvement. These include access to higher PZT
4
5 modulation frequency and improvement of the mirrors quality (a reflectivity
6
7 of 99.9%, in a larger bandwidth should be easily compatible with the actual
8
9 set-up).
10
11

12
13
14
15
16 Compared to CW-CRDS, sensitivity and resolution are not as high with
17
18 Femto-FT-CEAS but recording speed and spectral bandwidth are
19
20 significantly improved. Also, internal calibration procedure and data
21
22 processing is ensured by the FTIR software and readily available. The many
23
24 different possible recording conditions make a more quantitative comparison
25
26 between CRDS and Femto-FT-CEAS difficult. It is clear, for instance that
27
28 when combined to jet cooled experiments as used in our lab (28,29), both
29
30 would address different types of problems, the former to be focused on
31
32 exploring the absorption spectrum over a broad range, the latter to be
33
34 dedicated to high sensitivity and high resolution investigations.
35
36
37
38
39

40
41 Two of the major advantages of Femto-FT-CEAS using a broadband
42
43 OPO absorption source compared to more conventional FTIR approaches are
44
45 that (i) thanks to the source brightness, high quality data can be recorded in
46
47 a short amount of time, and (ii) the cell volume is much smaller (less than
48
49 200 cc in the present case) than for conventional multipass designs for
50
51 identical or even larger pathlengths. We actually hope to benefit from the
52
53 first of these by implementing Femto-FT-CEAS around the supersonic
54
55
56
57
58
59
60

1
2
3 expansion of FANTASIO+ in the very near future. We hope to exploit the
4
5 second advantage by recording NIR spectra of rare isotopologues, usually to
6
7 expensive to fill in a large multipass cell. Of particular relevance are all those
8
9 isotopologues of acetylene investigated in the MIR by Di Lonardo and co-
10
11 authors, including $^{12}\text{C}_2\text{HD}$ (35-39), $^{12}\text{CH}^{13}\text{CH}$ (40-50), $^{13}\text{C}_2\text{H}_2$ (40,41,51-55),
12
13 $^{12}\text{C}_2\text{D}_2$ (56-58), $^{13}\text{C}_2\text{D}_2$ (59-62), $^{13}\text{C}_2\text{HD}$ (63), $\text{H}^{12}\text{C}^{13}\text{CD}$ and $\text{H}^{13}\text{C}^{12}\text{CD}$ (64) (not
14
15 forgetting $^{12}\text{C}_2\text{H}_2$ (52,53,55,65,66)) for which the information could be
16
17 extended towards the NIR, with the help of the Bologna group.
18
19
20
21
22
23
24
25
26
27

28 **Acknowledgments**

29
30 We are happy to dedicate this paper to Prof. Di Lonardo, for his many
31
32 contributions to the acetylene spectroscopy, a dedication shared with all of us.
33
34 We thank B. Amyay and P. Van Poucke (ULB) for their help on various
35
36 items. We are indebted to the “programme Currien/Tournesol” collaboration
37
38 sponsored by “Wallonie Bruxelles international », F.R.S.-FNRS and “Région
39
40 Wallone”, and ‘Ministère des Affaires étrangères” and “Ministère de
41
42 l’Education Nationale, de la Recherche et de la Technologie” on the Belgian
43
44 and French sides, respectively. This work was also sponsored in Belgium, by
45
46 the Fonds National de la Recherche Scientifique (FNRS, contracts FRFC and
47
48 IISN) and the « Action de Recherches Concertées de la Communauté
49
50 française de Belgique ».
51
52
53
54
55
56
57
58
59
60

References

- (1) ST Ridgway, JW Brault: *Annu. Rev. Astron. Astrophys.* 22 (1984) 291-317.
- (2) JW Brault: *Philos. Trans. R. Soc. London, Ser. A* 307 (1982) 503-11.
- (3) HA Gobbie, G Roland, L Delbouille: *Nature (London, U. K.)* 191 (1961) 264-5.
- (4) L Delbouille, M Migeotte: *J. Opt. Soc. Am.* 50 (1960) 1305-7.
- (5) G Guelachvili: *Opt. Commun.* 8 (1973) 171-5.
- (6) M Betrencourt, M Morillon-Chapey, C Amiot, G Guelachvili: *J. Mol. Spectrosc.* 57 (1975) 402-15.
- (7) DJW Kendall, HL Buijs, JWC Johns: *J. Mol. Struct.* 79 (1982) 39-42.
- (8) M Herman, JWC Johns, ARW McKellar: *J. Mol. Spectrosc.* 95 (1982) 405-12.
- (9) J Kauppinen: *Appl Opt* 14 (1975) 1987-92.
- (10) J Kauppinen, M Taanila: *Commentat. Phys.-Math., Soc. Sci. Fenn.* 42 (1972) 318-19.
- (11) J Chazelas, J Pliva, A Valentin, L Henry: *J. Mol. Spectrosc.* 110 (1985) 326-38.
- (12) G Pierre, A Valentin, L Henry: *Can. J. Phys.* 62 (1984) 254-9.
- (13) BP Winnewisser, M Winnewisser: *Proc. SPIE-Int. Soc. Opt. Eng.* 1145 (1989) 28-33.

- 1
2
3
4
5
6
7
8
9
10
11
12
13
14
15
16
17
18
19
20
21
22
23
24
25
26
27
28
29
30
31
32
33
34
35
36
37
38
39
40
41
42
43
44
45
46
47
48
49
50
51
52
53
54
55
56
57
58
59
60
- (14) J Vogt, M Winnewisser, K Yamada, G Winnewisser: *Chem. Phys.* 83 (1984) 309-18.
- (15) ARW McKellar: *J. Mol. Spectrosc.* 262 (2010) 1-10.
- (16) J Mandon, G Guelachvili, N Picque, F Druon, P Georges: *Opt. Letters* 32 (2007) 1677-79.
- (17) J Mandon, G Guelachvili, N Picque: *Nature Photonics* (2009) 99-102.
- (18) J Orphal, AA Ruth: *Opt. Express* 16 (2008) 19232-43.
- (19) R Engeln, G Meijer: *Rev. Sci. Instrum.* 67 (1996) 2708-13.
- (20) R Engeln, E Van den Berg, G Meijer, L Lin, GMH Knippels, AFG Van der Meer: *Chem. Phys. Letters* 269 (1997) 293-97.
- (21) S Kassi, C Depiesse, M Herman, D Hurtmans: *Mol. Phys.* 101 (2003) 1155-63.
- (22) SM Hu, A Campargue, ZY Wu, Y Ding, AW Liu, QS Zhu: *Chem. Phys. Letters* 372 (2003) 659-67.
- (23) S Kassi, K Didriche, C Lauzin, X de Ghellinck d'Elseghem Vaernewijck, A Rizopoulos, M Herman: *Spectrochim. Acta, A* 75A (2010) 142-45.
- (24) B Bernhardt, A Ozawa, P Jacquet, M Jacquy, Y Kobayashi, T Udem, R Holzwarth, G Guelachvili, TW Haensch, N Picque: *Nat. Photonics* 4 (2009) 55-57.
- (25) T Gherman, S Kassi, A Campargue, D Romanini: *Chem. Phys. Letters* 383 (2004) 353-58.

- 1
2
3 (26) T Gherman, D Romanini: *Optics Express* 10 (2002) 1033-42.
4
5
6 (27) M Herman, K Didriche, D Hurtmans, B Kizil, P Macko, A Rizopoulos,
7
8 P Van Poucke: *Mol. Phys.* 105 (2007) 815-23.
9
10 (28) K Didriche, C Lauzin, T Foldes, X. de Ghellinck d'Elseghem
11
12 Vaernewijck, M Herman: *Mol. Phys.* 108 (2010) 2155-63.
13
14 (29) K Didriche, C Lauzin, T Foldes, D Golebiowski, M Herman, C
15
16 Leforestier: *PCCP* doi: 10.1039/c1cp2059561g (2011).
17
18 (30) B Amyay, M Herman, A Fayt, A Campargue, S Kassi: *J. Mol.*
19
20 *Spectrosc.* doi:10.1016/j.jms.2011.02.015 (2011).
21
22 (31) BC Smith, JS Winn: *J. Chem. Phys.* 89 (1988) 4638-45.
23
24 (32) Q Kou, G Guelachvili, M Abbouti Temsamani, M Herman: *Can. J.*
25
26 *Phys.* 72 (1994) 1241-50.
27
28 (33) KA Keppler, GC Mellau, S Klee, BP Winnewisser, M Winnewisser, J
29
30 Plíva, KN Rao: *J. Mol. Spectrosc.* 175 (1996) 411-20.
31
32 (34) S Robert, M Herman, A Fayt, A Campargue, S Kassi, A Liu, L Wang, G
33
34 Di Lonardo, L Fusina: *Mol. Phys.* 106 (2008) 2581-605.
35
36 (35) M Herman, C Depiesse, G Di Lonardo, A Fayt, L Fusina, D Hurtmans,
37
38 S Kassi, M Mollabashi, J Vander Auwera: *J. Mol. Spectrosc.* 228 (2004)
39
40 499-510.
41
42 (36) L Fusina, E Cane, F Tamassia, G Di Lonardo: *Mol. Phys.* 103 (2005)
43
44 3263-70.
45
46 (37) L Fusina, F Tamassia, G Di Lonardo: *Mol. Phys.* 103 (2005) 2613-20.
47
48
49
50
51
52
53
54
55
56
57
58
59
60

- 1
2
3
4
5
6
7
8
9
10
11
12
13
14
15
16
17
18
19
20
21
22
23
24
25
26
27
28
29
30
31
32
33
34
35
36
37
38
39
40
41
42
43
44
45
46
47
48
49
50
51
52
53
54
55
56
57
58
59
60
- (38) A Jolly, Y Benilan, E Cané, L Fusina, F Tamassia, A Fayt, S Robert, M Herman: *J. Quant. Spectrosc. Radiat. Transfer* 109 (2008) 2846-56.
- (39) A Predoi-Cross, M Herman, L Fusina, G Di Lonardo: *Mol. Phys.* 109 (2011) 559-63.
- (40) G Di Lonardo, P Ferracuti, L Fusina, E Venuti, JWC Johns: *J. Mol. Spectrosc.* 161 (1993) 466-86.
- (41) G Di Lonardo, P Ferracuti, L Fusina, E Venuti: *J. Mol. Spectrosc.* 164 (1994) 219-32.
- (42) F Alboni, G Di Lonardo, P Ferracuti, L Fusina, E Venuti, KA Mohamed: *J. Mol. Spectrosc.* 169 (1995) 148-53.
- (43) G Di Lonardo, A Baldan, G Bramati, L Fusina: *J. Mol. Spectrosc.* 213 (2002) 57-63.
- (44) L Fusina, G Bramati, A Mazzavillani, G Di Lonardo: *Mol. Phys.* 101 (2002) 513-21.
- (45) C Depiesse, G Di Lonardo, A Fayt, L Fusina, D Hurtmans, S Robert, F Tamassia, J Vander Auwera, A Baldan, M Herman: *J. Mol. Spectrosc.* 229 (2005) 137-39.
- (46) S Robert, A Fayt, G Di Lonardo, L Fusina, F Tamassia, M Herman: *J. Chem Phys* 123 (2005) 174302.
- (47) G Di Lonardo, L Fusina, F Tamassia, A Fayt, S Robert, J Vander Auwera, M Herman: *Mol. Phys.* 104 (2006) 2617-25.

- 1
2
3 (48) A Fayt, S Robert, G Di Lonardo, L Fusina, F Tamassia, M Herman: J.
4
5 Chem. Phys. 126 (2007) 114303.
6
7
8 (49) G Di Lonardo, L Fusina, F Tamassia, A Fayt, S Robert, J Vander
9
10 Auwera, M Herman: Mol. Phys. 106 (2008) 1161-69.
11
12 (50) S Robert, B Amyay, A Fayt, G Di Lonardo, L Fusina, F Tamassia, M
13
14 Herman: J Phys Chem A 113 (2009) 13251-9.
15
16
17 (51) E Venuti, G Di Lonardo, P Ferracuti, L Fusina, IM Mills: Chem. Phys.
18
19 190 (1995) 279-90.
20
21
22 (52) M Becucci, E Castellucci, L Fusina, G Di Lonardo, HW Schrotter: J.
23
24 Raman Spectrosc. 29 (1998) 237-41.
25
26
27 (53) D Bermejo, P Cancio, G Di Lonardo, L Fusina: J. Chem. Phys. 108
28
29 (1998) 7224-28.
30
31
32 (54) G Di Lonardo, L Fusina, E Venuti, JWC Johns, MI El Idrissi, J Liévin,
33
34 M Herman: J. Chem. Phys. 111 (1999) 1008-16.
35
36
37 (55) D Bermejo, RZ Martinez, G Di Lonardo, L Fusina: J. Chem. Phys. 111
38
39 (1999) 519-24.
40
41
42 (56) M Herman, IMI El, A Pisarchik, A Campargue, AC Gaillot, L Biennier,
43
44 G Di Lonardo, L Fusina: J. Chem. Phys. 108 (1998) 1377-89.
45
46
47 (57) D Bermejo, G Di Lonardo, JL Doménech, L Fusina: J. Mol. Spectrosc.
48
49 209 (2001) 259-66.
50
51
52 (58) S Robert, M Herman, J Vander Auwera, G Di Lonardo, L Fusina, G
53
54 Blanquet, M Lepere, A Fayt: Mol. Phys. 105 (2007) 559-68.
55
56
57
58
59
60

- 1
2
3
4
5
6
7
8
9
10
11
12
13
14
15
16
17
18
19
20
21
22
23
24
25
26
27
28
29
30
31
32
33
34
35
36
37
38
39
40
41
42
43
44
45
46
47
48
49
50
51
52
53
54
55
56
57
58
59
60
- (59) E Cane, G Cazzoli, G Di Lonardo, L Dore, R Escribano, L Fusina: J. Mol. Spectrosc. 216 (2002) 447-53.
- (60) D Bermejo, G Di Lonardo, JL Doménech, L Fusina: Mol. Phys. 100 (2002) 3493-97.
- (61) D Bermejo, G Di Lonardo, JL Domenech, L Fusina: Mol. Phys. 101 (2003) 3203-12.
- (62) D Bermejo, G Di Lonardo, JL Domenech, L Fusina: J. Mol. Spectrosc. 219 (2003) 290-95.
- (63) L Fusina, F Tamassia, G Di Lonardo, A Baldan: Mol. Phys. 107 (2009) 2119-26.
- (64) L Fusina, E Cané, F Tamassia, G Di Lonardo: Mol. Phys. 105 (2007) 2321 – 25.
- (65) Y Kabbadj, M Herman, G Di Lonardo, L Fusina, JWC Johns: J. Mol. Spectrosc. 150 (1991) 535-65.
- (66) S Robert, M Herman, A Fayt, A Campargue, S Kassi, A Liu, L Wang, G Di Lonardo, L Fusina: Mol. Phys. 106 (2008) 2581-605.

Figure captions

Figure 1: Illustration of the broad spectral coverage using a femto OPO absorption source and FTIR, in the NIR portion of the OPO emission. Absorption lines are from atmospheric water. OPO emission has 90 cm^{-1} FWHM spectral coverage in the lower energy range.

Figure 2: FTIR absorption spectrum of $\nu_1+\nu_3$, C_2H_2 recorded using FANTASIO+, a multipass optics set to 25 passes and a femto OPO absorption source. Input and output pressures around the 0.5mm circular nozzle: 1355 Torr and 14 mTorr, respectively; Flow rates: 2,2 l/min (C_2H_2) and 1,8 l/min (Ar, carrier gas); FTIR resolution: $3 \cdot 10^{-2} \text{ cm}^{-1}$.

Figure 3: FTIR absorption spectrum of $\nu_1+\nu_3$, C_2H_2 recorded using off-axis CEAS design and a femto OPO absorption source (top), compared to simulation (bottom) (saturated peaks were removed from the data points). Experimental conditions: P: 2 Torr; FTIR resolution: 0.005 cm^{-1} ; Absorption pathlength: 5 m.

Figure 4: Experimental design for Femto-FT-CEAS using an OPO tunable source. Laser: Chameleon Ultra II, P810 OPO Signal or Idler; OI: optical isolator; M1, L1, L2, M3, M4, L3: steering optics; CM1, CM2:

1
2
3 high reflective cavity mirrors (99.5%); FTIR: Bruker IFS 120 HR; PZT:
4
5
6 Piezoelectric modulator.
7
8
9

10
11 *Figure 5:* FTIR absorption spectrum (arbitrary intensity units) of a femto
12
13 OPO source injected in a high finesse cavity for various PZT
14
15 modulation frequencies: 0, 20, 200, 2000, 20000 Hz from top to bottom.
16
17
18 Experimental conditions: Resolution: 0.02 cm^{-1} ; 10 accumulated scans.
19
20
21
22

23
24 *Figure 6:* Portion of the Femto-FT-CEAS spectrum of $\nu_1+\nu_3$, C_2H_2 recorded
25
26 using an OPO absorption source, for various FTIR resolutions: 0.04,
27
28 0.02, 0.01, 0.005 cm^{-1} from bottom to top.
29
30
31 Experimental conditions: P: 2 Torr; Absorption pathlength: 150 m; 10
32
33 accumulated scans.
34
35
36
37

38
39 *Figure 7:* FTIR spectrum of $\nu_1+\nu_3$, C_2H_2 recorded using CEAS design and a
40
41 femto OPO absorption source (saturated peaks were removed from the
42
43 data points). Experimental conditions: P: 10 Torr; FTIR resolution:
44
45 0.02 cm^{-1} ; 180 accumulated scans.
46
47
48
49
50

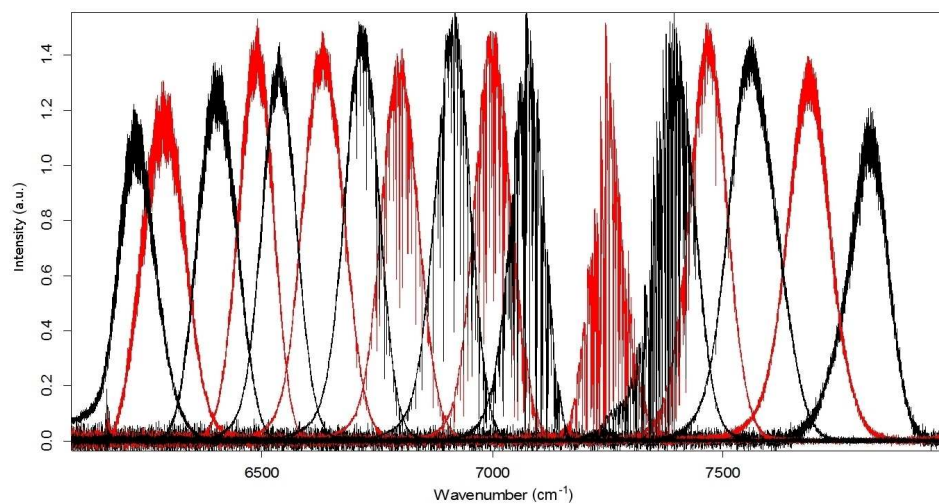
51
52 *Figure 8:* Portions of the spectrum of $\nu_1+\nu_3$, C_2H_2 shown on Figure 8. Newly
53
54 assigned R and P transitions are indicated by arrows. Top/bottom figures
55
56 highlight (a)/(b) bands identified in Table 1, respectively.
57
58
59
60

Table 1

Calc.	Ass.	Obs.	Obs.-Calc.
(a) 1 1 0 2 2, 2 0 eg - 0 0 0 1 1, 1 1 eu			
6557.324	P5	6557.330	0.006
6583.118	R5	6583.104	-0.014
6589.857	R8	6589.849	-0.008
6596.499	R11	6596.493	-0.006
6598.695	R12	6598.685	-0.010
(b) 1 1 0 2 2, 2 -2 eg - 0 0 0 1 1, 1 -1			
6547.532	P10	6547.538	0.006
6552.536	P8	6552.530	-0.006
6557.466	P6	6557.460	-0.006
6559.906	P5	6559.903	-0.003
6562.329	P4	6562.327	-0.001
6578.854	R2	6578.850	-0.004
6581.152	R3	6581.153	0.001
6587.939	R6	6587.923	-0.016
6590.163	R7	6590.163	0.000
6592.366	R8	6592.360	-0.006
6596.705	R10	6596.691	-0.014

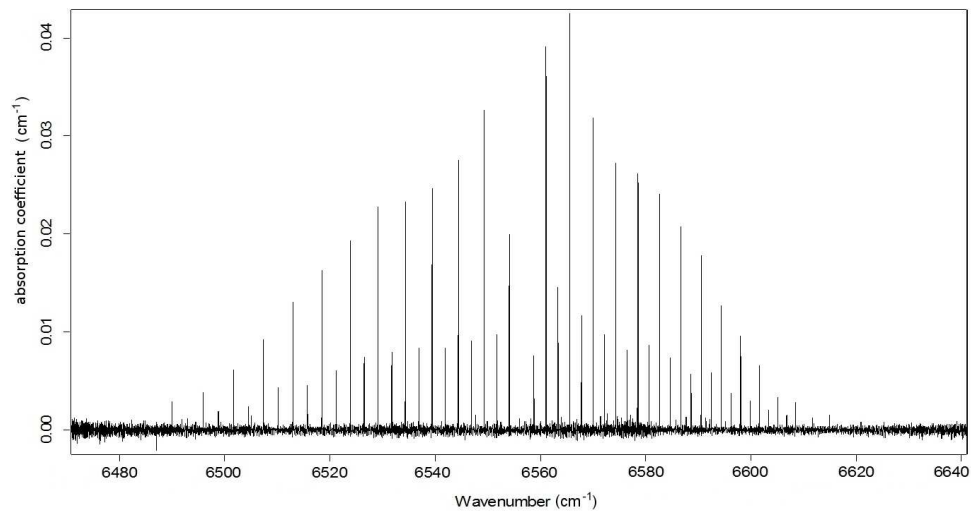
Table caption*Table 1*

Transitions assigned in $^{12}\text{C}_2\text{H}_2$. The bands are identified using conventional numbering (30): $v_1 v_2 v_3 v_4 v_5, l_4 l_5 e/f, u/g$. The predicted line wavenumbers (from (30)), rotational assignments, observed and observed-predicted wavenumbers (all positions in cm^{-1}) are provided.



508x264mm (72 x 72 DPI)

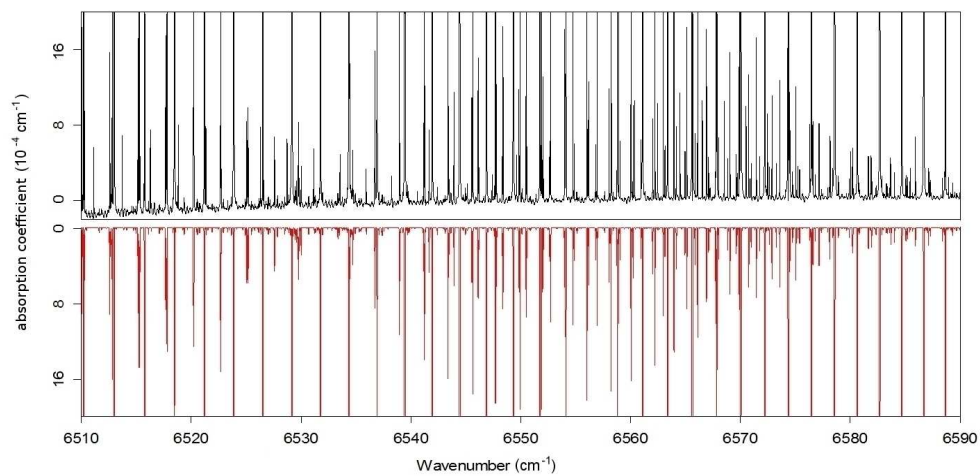
Review Only



498x258mm (72 x 72 DPI)

Review Only

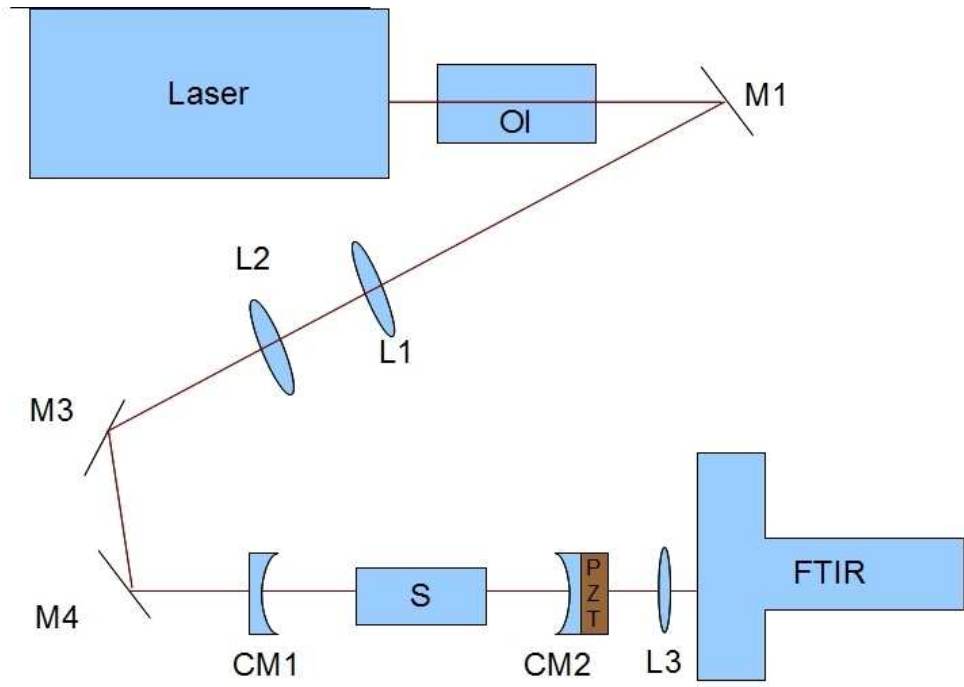
1
2
3
4
5
6
7
8
9
10
11
12
13
14
15
16
17
18
19
20
21
22
23
24
25
26
27
28
29
30
31
32
33
34
35
36
37
38
39
40
41
42
43
44
45
46
47
48
49
50
51
52
53
54
55
56
57
58
59
60



508x246mm (72 x 72 DPI)

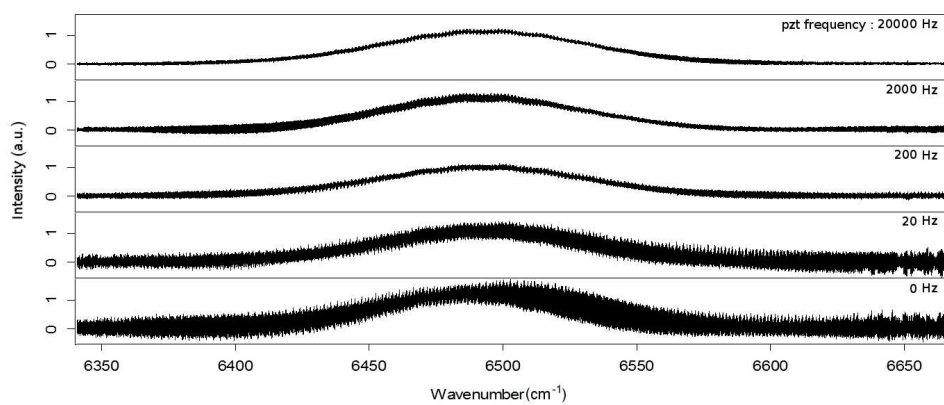
Review Only

1
2
3
4
5
6
7
8
9
10
11
12
13
14
15
16
17
18
19
20
21
22
23
24
25
26
27
28
29
30
31
32
33
34
35
36
37
38
39
40
41
42
43
44
45
46
47
48
49
50
51
52
53
54
55
56
57
58
59
60



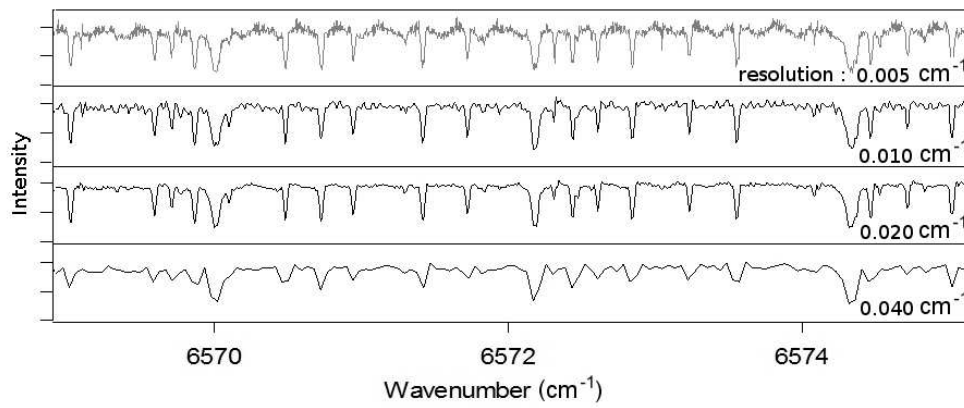
261x186mm (72 x 72 DPI)

view Only



508x211mm (72 x 72 DPI)

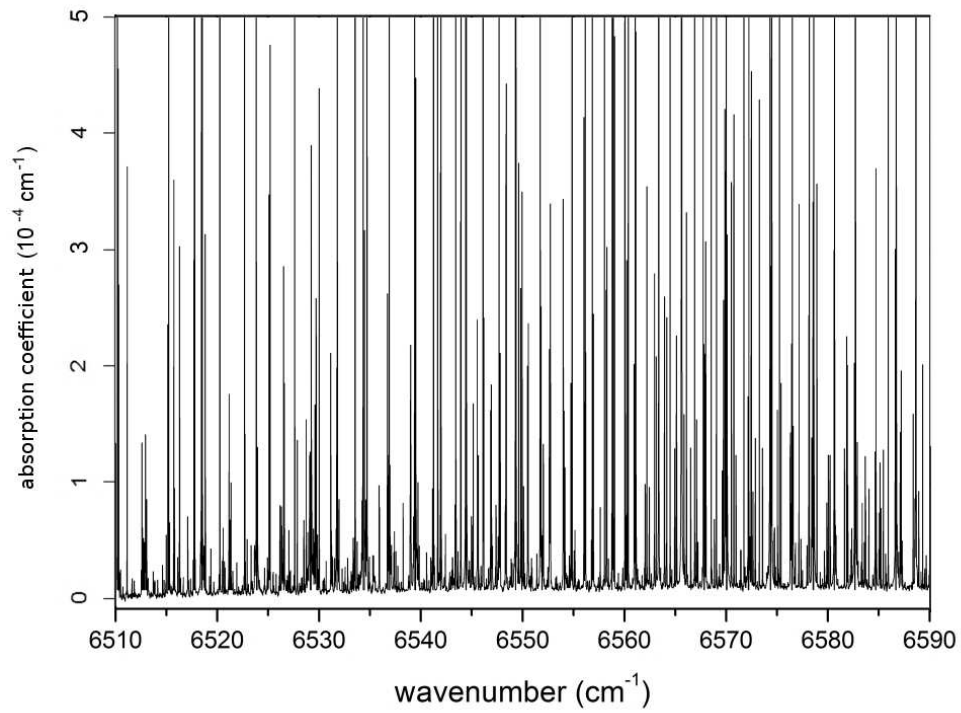
Peer Review Only



324x139mm (72 x 72 DPI)

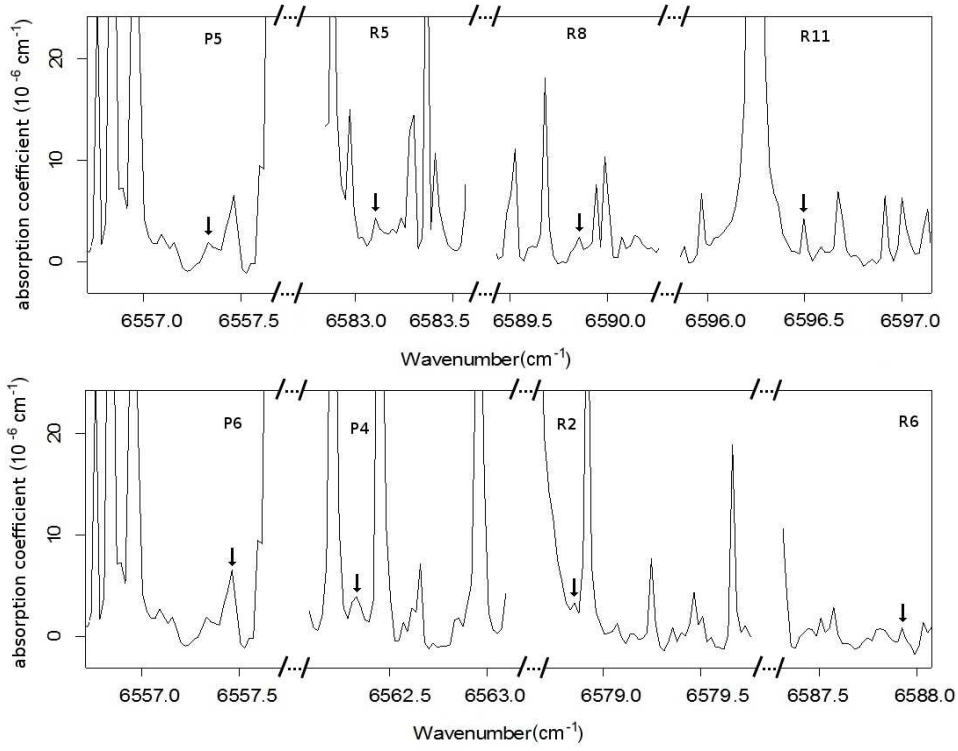
Peer Review Only

1
2
3
4
5
6
7
8
9
10
11
12
13
14
15
16
17
18
19
20
21
22
23
24
25
26
27
28
29
30
31
32
33
34
35
36
37
38
39
40
41
42
43
44
45
46
47
48
49
50
51
52
53
54
55
56
57
58
59
60



83x63mm (300 x 300 DPI)

View Only



402x317mm (72 x 72 DPI)

new Only

1
2
3
4
5
6
7
8
9
10
11
12
13
14
15
16
17
18
19
20
21
22
23
24
25
26
27
28
29
30
31
32
33
34
35
36
37
38
39
40
41
42
43
44
45
46
47
48
49
50
51
52
53
54
55
56
57
58
59
60